International Journal of Biological Macromolecules 163 (2020) 1649–1658

Contents lists available at ScienceDirect

International Journal of Biological Macromolecules

journal homepage: http://www.elsevier.com/locate/ijbiomac

# The structure-activity relationship of the interactions of SARS-CoV-2 spike glycoproteins with glucuronomannan and sulfated galactofucan from *Saccharina japonica*

Weihua Jin [a,b,*], Wenjing Zhang [c], Dipanwita Mitra [e], Martin G. McCandless [e], Poonam Sharma [e], Ritesh Tandon [e], Fuming Zhang [b,**], Robert J. Linhardt [b,d,***]

[a] College of Biotechnology and Bioengineering, Zhejiang University of Technology, Hangzhou 310014, China
[b] Department of Chemical and Biological Engineering, Center for Biotechnology and Interdisciplinary Studies, Rensselaer Polytechnic Institute, Troy, NY 12180, USA
[c] Department of Endocrinology, Sir Run Run Shaw Hospital, Zhejiang University School of Medicine, Hangzhou 310016, China
[d] Departments of Biological Science, Chemistry and Chemical Biology and Biomedical Engineering, Center for Biotechnology and Interdisciplinary Studies, Rensselaer Polytechnic Institute, Troy, NY 12180, USA
[e] Department of Microbiology and Immunology, University of Mississippi Medical Center, Jackson, MS 39216, USA

ARTICLE INFO

*Article history:*
Received 23 July 2020
Received in revised form 8 September 2020
Accepted 21 September 2020
Available online 24 September 2020

*Keywords:*
Glucuronomannan
Sulfated galactofucan
SARS-CoV-2

ABSTRACT

The SARS-CoV-2 spike glycoproteins (SGPs) and human angiotensin converting enzyme 2 (ACE2) are the two key targets for the prevention and treatment of COVID-19. Host cell surface heparan sulfate (HS) is believed to interact with SARS-CoV-2 SGPs to facilitate host cell entry. In the current study, a series of polysaccharides from *Saccharina japonica* were prepared to investigate the structure-activity relationship on the binding abilities of polysaccharides (oligosaccharides) to pseudotype particles, including SARS-CoV-2 SGPs, and ACE2 using surface plasmon resonance. Sulfated galactofucan (SJ-D-S-H) and glucuronomannan (Gn) displayed strongly inhibited interaction between SARS-CoV-2 SGPs and heparin while showing negligible inhibition of the interaction between SARS-CoV-2 SGPs and ACE2. The $IC_{50}$ values of SJ-D-S-H and Gn in blocking heparin SGP binding were 27 and 231 nM, respectively. NMR analysis showed that the structure of SJ-D-S-H featured with a backbone of 1, 3-linked α-L-Fuc*p* residues sulfated at C4 and C2/C4 and 1, 3-linked α-L-Fuc*p* residues sulfated at C4 and branched with 1, 6-linked β-D-galacto-biose; Gn had a backbone of alternating 1, 4-linked β-D-GlcA*p* residues and 1, 2-linked α-D-Man*p* residues. The sulfated galactofucan and glucuronomannan showed strong binding ability to SARS-CoV-2 SGPs, suggesting that these polysaccharides might be good candidates for preventing and/or treating SARS-CoV-2.



## 1. Introduction

COVID-19, caused by the SARS-CoV-2 virus, has now spread worldwide with the tremendous human and economic impact. SARS-CoV-2 is a zoonotic betacoronarirus transmitted through person to person contact by airborne and fecal-oral routes [1]. Approximately 15 million cases of COVID-19 and more than 600,000 deaths have been reported [2]. The absence of vaccines prompts the need for antiviral therapeutics.

Previous studies [3–5] have shown that the host cell surface glycosaminoglycan (GAG), heparan sulfate (HS), interacts with SARS-CoV-2 spike glycoprotein (SGP) and may facilitate host cell entry. Surface plasmon resonance (SPR) has been performed to detect the binding ability between SGP and heparin, a highly sulfated HS analog. Monomeric SARS-CoV-2 SGP was shown to bind more tightly to immobilized heparin ($K_D = 40$ pM) than did SARS-CoV SGP (500 nM) and MERS-CoV SGP (1 nM) [3]. The results of the competition binding assay indicated that the $IC_{50}$ of heparin, tri-sulfated non-anticoagulant HS and low molecular weight heparin were 0.056 μM, 0.12 μM, and 26.4 μM, respectively [3]. In addition, unbiased computational ligand docking studies suggested that the heparan sulfate (HS) binding domains were at the subunit 1 (S1)/subunit 2 (S2) of spike glycoprotein site and another site (453-459 (YRLFRKS)) [3].

Sulfated polysaccharides from brown seaweeds have similar structures to GAGs. Compared to heparin, the polysaccharide (RPI-27) and

* Correspondence to: W. Jin, College of Biotechnology and Bioengineering, Zhejiang University of Technology, Hangzhou 310014, China.
** Corresponding author.
*** Correspondence to: R.J. Linhardt, Departments of Biological Science, Chemistry and Chemical Biology and Biomedical Engineering, Center for Biotechnology and Interdisciplinary Studies, Rensselaer Polytechnic Institute, Troy, NY 12180, USA.
*E-mail addresses:* jinweihua@zjut.edu.cn (W. Jin), zhangf2@rpi.edu (F. Zhang), linhar@rpi.edu (R.J. Linhardt).

https://doi.org/10.1016/j.ijbiomac.2020.09.184
0141-8130/

low molecular weight polysaccharide (RPI-28), from *Saccharina japonica*, were shown to exhibit and strongly inhibit the binding of SARS-CoV-2 SGP to immobilized heparin [6]. In addition, RPI-27 and RPI-28 did not show any toxicity using Vero cells using a standard water-soluble tetrazolium salt-1 (WST-1) assay, even at the highest concentrations studied. Moreover, in an *in vitro* antiviral assays, RPI-28 had an $EC_{50}$ of 8.3 ± 4.6 μg/mL (corresponding to approximately 83 nM) [6], and was more potent than remdesivir (a drug recently approved for emergency use in severe COVID-19 infections), heparin (2.1 μM), chemo-enzymatically synthesized TriS (a non-anticoagulant heparin analog) [7] (5.0 μM) and non-anticoagulant low molecular weight (LMW) heparin (NACH) [8] (55 μM). These strong interactions were attributed to multivalent binding between the polysaccharides and the SGPs of viral particles [9].

Due to the highly transmissible and pathogenic nature of SARS-CoV-2, a biosafety level 3 (BSL3) containment is required for live-virus studies [10]. A pseudotyping system, which mimics the surface properties of SARS-CoV-2, has been used in biosafety level 2 (BSL2) laboratories for the purpose of vaccine studies, drug inhibition studies and serological screening [10]. Recently, a sulfated fucan from *Lytechinus variegatus* (sea urchin) and a sulfated galactan from *Botryocladia occidentalis* (red seaweed) were found to have anti-SARS-CoV-2 activity using these pseudotype SARS-CoV-2 particles [11]. SARS-CoV-2 SGFs could bind ACE2 based on previous studies [12]. In the current study, interactions between pseudotyped particles and polysaccharides from *Saccharina japonica* have been further investigated to elucidate their structure-activity relationship. In addition, the possible inhibitory activities of polysaccharides on the interaction between SARS-CoV-2 SGPs and ACE2 were also determined.

## 2. Materials and methods

### 2.1. Preparation of polysaccharides from Saccharina japonica

Crude polysaccharide from *Saccharina japonica* (SJ) was obtained according to a previous study by hot water extraction [13]. SJ-100K, SJ-50K, SJ-30K, SJ-10K and SJ-3K were prepared from 0.2 M formic acid catalyzed degradation of SJ using five types of ultrafiltration devices (Ultracel 100 kDa membrane, Ultracel 50 kDa membrane, Ultracel 30 kDa membrane, Ultracel 10 kDa membrane and Ultracel 3 kDa membrane, respectively (Sigma-Aldrich)) [14]. LMW polysaccharide (SJ-D) was prepared by the degradation of SJ polysaccharide using hydrogen peroxide and ascorbic acid [14–17]. SJ and SJ-D were separated by anion-exchange chromatography on a DEAE-Bio Gel agarose FF (6 cm × 40 cm) eluted with water (5 L), 0.5 M NaCl (5 L) (Fraction W: SJ-W and SJ-D-W), 1 M NaCl (5 L) (Fraction I: SJ-I and SJ-D-I) and 2 M NaCl (5 L) (Fraction S: SJ-S and SJ-D-S) [14]. Autohydrolysis was carried out by methods described in previous studies [18–24]. Two types of autohydrolyzed polysaccharides, including higher molecular weight, H-type fractions (SJ-D-W-H, SJ-D-I-H and SJ-D-S-H) and lower molecular weight, L-type fractions (SJ-D-W-L, SJ-D-I-L and SJ-D-S-L) were obtained [14]. Glucuronomannan oligomers (G2, G4 and G6, disaccharide, tetrasaccharide and hexasaccharide, respectively) and glucuronomannan polysaccharide (Gn) with a molecular weight of 7.0 kDa were prepared in our laboratory by previously described methods [25–27]. The desulfated polysaccharides (SJ-I-DS, SJ-S-DS, SJ-D-I-DS and SJ-D-S-DS) and oversulfated polysaccharides (SJ-I-PS, SJ-S-PS, SJ-D-I-PS and SJ-D-S-PS) were prepared according to the previous studies [13,14,28]. Acid degradation was carried out according to the previous study [29]. Three fractions were obtained. Briefly, crude polysaccharide (10 mg/mL) was dissolved in 0.1 M HCl and stirred for 0.5 h at 80 °C. The mixture was neutralized with 5% $NH_4OH$ solution in water. The solution was concentrated and precipitated by ethanol. The supernatant (Fraction GX-1: SJ-GX-1 and SJ-D-W-GX-1) was dialyzed and lyophilized. The precipitant was further degraded by 0.5 M HCl and stirred for 2 h at 80 °C. The mixture was neutralized with 5% $NH_4OH$ solution in water. The solution was concentrated and precipitated by ethanol. The supernatant (Fraction GX-2: SJ-GX-2 and SJ-D-W-GX-2) was dialyzed and lyophilized. The precipitants (Fraction GX-3: SJ-GX-3 and SJ-D-W-GX-3) were then dialyzed and lyophilized. All samples studied were summarized in Scheme 1.

### 2.2. Solution competition SPR analysis

Solution competition SPR measurements were performed on a BIAcore 3000 (GE Healthcare, Uppsala, Sweden). A heparin chip was prepared based on previous studies [5] by the immobilization of biotinylated heparin on a streptavidin (SA) chip. Pseudotype particles were prepared as in previous studies [10,11]. Briefly, HEK293T cells (2 × 106) were plated in a 100-mm tissue culture dish and transfected the next day

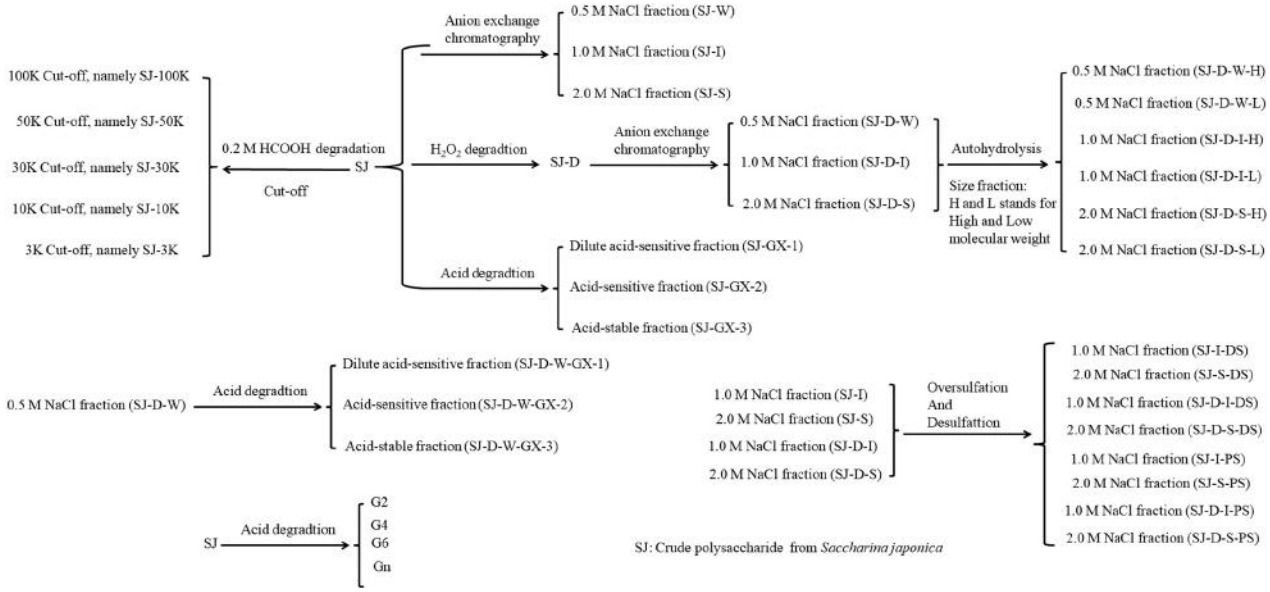


**Scheme 1.** The flow chart of sample preparation.

with a combination of the following plasmids: 9 μg of pLV-eGFP, 9 μg of psPAX2, and 3 μg of pCAGGS-S (SARS-CoV-2)(Catalog No. NR-52310: BEI-Resources). The supernatant from cell culture was harvested, spun in a tabletop centrifuge for 5 min at 2000 ×*g* to pellet the residual cells and then passed through a 0.45 μm syringe filter. Virus titers were calculated by plating on new HEK293T cells and enumerating GFP positive cells. Pseudotype particles were pre-mixed with different concentrations of polysaccharides or oligosaccharides in HBS-EP buffer and injected over the heparin chip at 30 μL/min to measure the inhibition of pseudotype particle binding to heparin surface. After each run, there was a dissociation period of 3 min and a regeneration period of 1 min using 2 M NaCl.

SARS-CoV-2 spike protein was purchased from Sino Biological Inc. (catalog #: 40591-V02H). SARS-CoV-2 spike protein was immobilized covalently to a CM5 sensor chip using manufacturer methods. Human angiotensin converting enzyme 2 (ACE2 was a generous gift from Professor Jason McLellan from the University of Texas at Austin) at 500 nM with or without polysaccharides or oligosaccharides was injected over the SARS-CoV-2 spike protein chip at 30 μL/min to measure the inhibition of polysaccharides or oligosaccharides on ACE2 binding to SARS-CoV-2 spike protein chip. After each run there was a dissociation period of 3 min and regeneration period of 1 min using with 2 M NaCl.

### *2.3. Compositional analysis and nuclear magnetic resonance (NMR) spectroscopy*

The molar ratio of monosaccharides, fucose (Fuc) and galactose (Gal) contents, were determined based on a modified method from a previous study [30]. Sulfate content was determined by the paper of Dodgson and Price [31]. The molecular weights of the polysaccharides were determined using gel permeation chromatography-high performance liquid chromatography (GPC-HPLC) on TSK G3000 PWxl column (7 μm, 7.8 × 300 mm) with elution in 0.05 M $Na_2SO_4$ at a flow rate of 0.5 mL/min at 40 °C with refractive index detection. Ten different molecular weight dextrans, purchased from the National Institute for the Control of Pharmaceutical and Biological Products (China), were used as molecular weight standards.

For NMR analysis, polysaccharides (30 mg) were co-evaporated with deuterium oxide (99.9%) twice before dissolving in deuterium oxide. One-and two-dimensional spectra, including $^{1}H$ NMR, $^{13}C$ NMR and $^{1}H$—$^{13}C$ heteronuclear single quantum coherence spectroscopy (HSQC), were recorded at a Hudson-Bruker SB 800 MHz spectrometer (Bruker BioSpin, Billerica, MA, USA) at 25 °C.

## 3. Results

### *3.1. SPR solution competition study of different polysaccharides obtained by anion exchange chromatography on heparin chip*

According to a previous study [6], polysaccharide (SJ) from *Saccharina japonica* has anti-SARS-CoV-2 virus activity and exhibits stronger inhibitory activity binding to SARS-CoV-2 SGPs. Therefore, SJ and its derivatives were screened using SPR to determine binding affinity to the pseudotype particles for the purpose of structure-activity relationship. SJ showed the strongest inhibitory activity, which was consistent with the previous study (Fig. 1A). Molecular weight influenced the binding ability, however, SJ-D still exhibited a strong inhibitory activity (>80%) (Fig. 1B). Anion exchange chromatography was carried out to separate SJ and SJ-D and SJ-I, SI-S and SJ-D-S showed strong inhibitory activity (>80%). Previous studies [15–17] showed that SJ-I, SI-S and SJ-D-S were sulfated galactofucans.

### *3.2. SPR solution competition study on modified polysaccharides (mainly sulfated galactofucans) using a heparin chip*

After autohydrolysis, two fractions (H-type fraction with high molecular weight and L-type fraction with low molecular weight) were

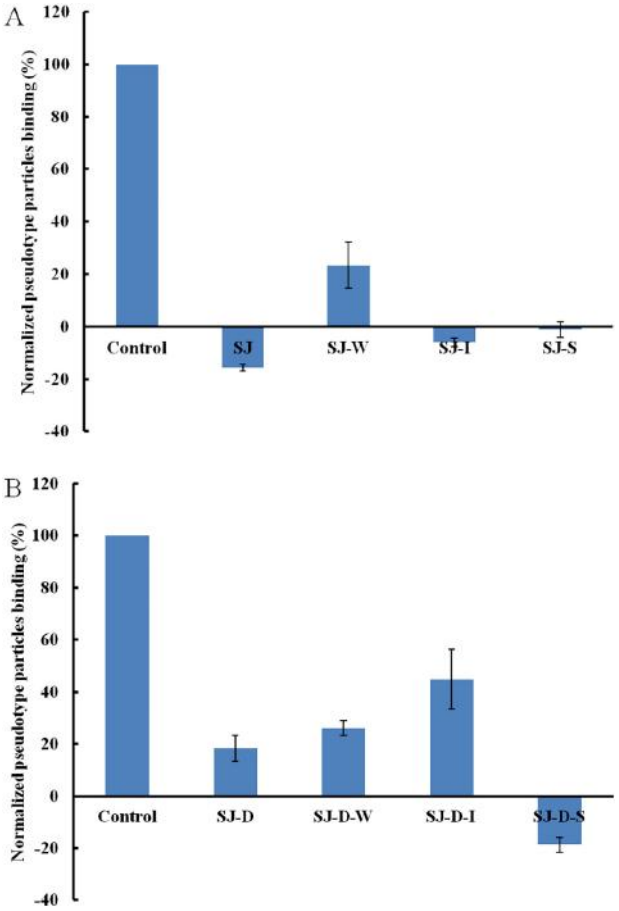


**Fig. 1.** Bar graphs of normalized pseudotype particles binding preference to surface heparin by competing with SJ and its fractions (A) and SJ-D and its fractions (B). Concentration of pseudotype particles was 0.085 mg/mL and concentrations of different polysaccharides were 1000 nM. All bar graphs with standard deviations were based on triplicate experiments.

obtained. The results of SPR (Fig. 2A) indicated that H-type fractions (SJ-D-W-H, SJ-D-I-H and SJ-D-S-H) had stronger inhibitory activities than L-type fractions (SJ-D-W-L, SJ-D-I-L and SJ-D-S-L). SJ-D-I-H and SJ-D-S-H showed strong inhibitory activity (> 80%). The impact of sulfate was examined using desulfated polysaccharides (SJ-I-DS, SI-S-DS, SJ-D-I-DS and SJ-D-S-DS) and chemically oversulfated polysaccharides (SJ-I-PS, SI-S-PS, SJ-D-I-PS and SJ-D-S-PS). Oversulfated polysaccharides exhibited very strong inhibitory activities, which were stronger than the native polysaccharides (Fig. 2B and C). Desulfated polysaccharides exhibited only very weak or no inhibitory activities and were weaker inhibitors than the native polysaccharides. We conclude that the presence of sulfate groups a one-factor influencing polysaccharide binding to pseudotype particles.

### *3.3. SPR solution competition study on modified polysaccharides (mainly on glucuronomannan) on heparin chip*

Five MWCO membranes (100 K, 50 K, 30 K, 10 K and 3 K) were used to separate the partially degraded polysaccharides by 0.2 M formic acid. SJ-100 K showed the strongest inhibitory activity (Fig. 3A). In addition, 0.1 M HCl and 0.5 M HCl were used sequentially to degrade SJ and SJ-D-W to obtain three fractions: (1) dilute acid-sensitive fractions (SJ-GX-1 and SJ-D-W-GX-1); (2) acid-sensitive fractions (SJ-GX-2 and SJ-D-W-GX-2); and (3) acid-stable fractions (SJ-GX-3 and SJ-D-W-GX-3), respectively. Acid-

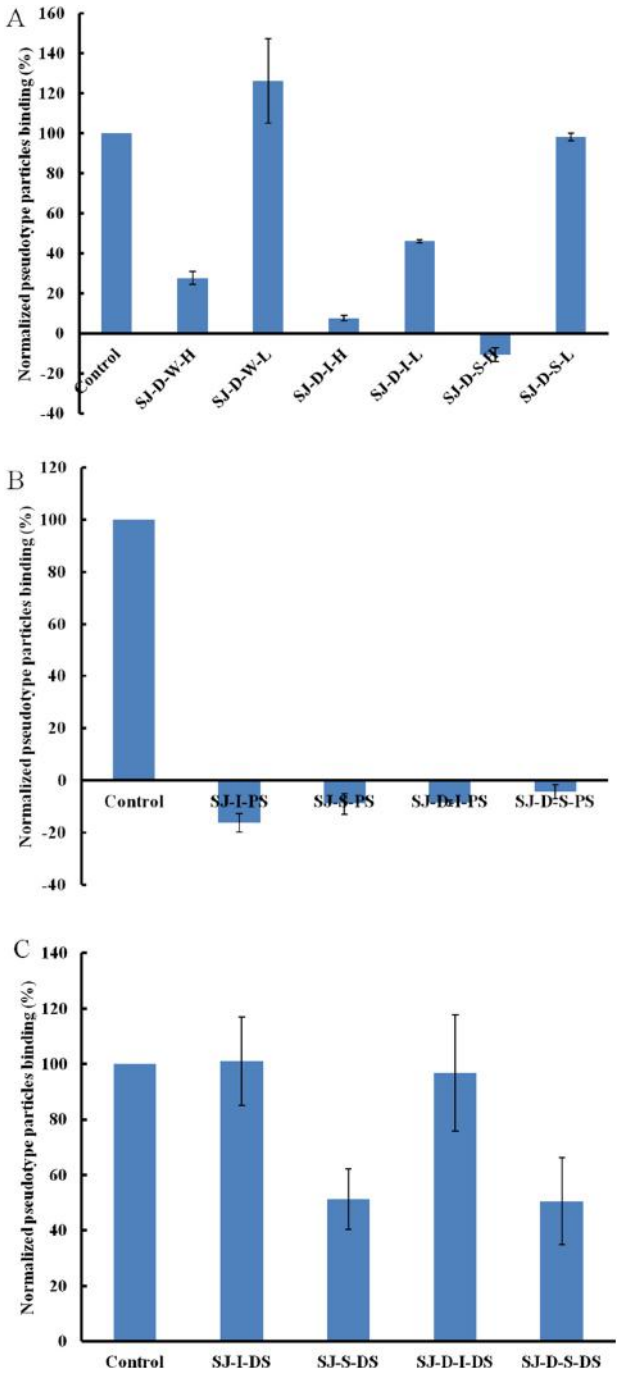


**Fig. 2.** Bar graphs of normalized pseudotype particles binding preference to surface heparin by competing with different modified polysaccharides (mainly on sulfated galactofucan). Concentration of pseudotype particles was 0.085 mg/mL and concentrations of different polysaccharides were 1000 nM. All bar graphs with standard deviations were based on triplicate experiments.

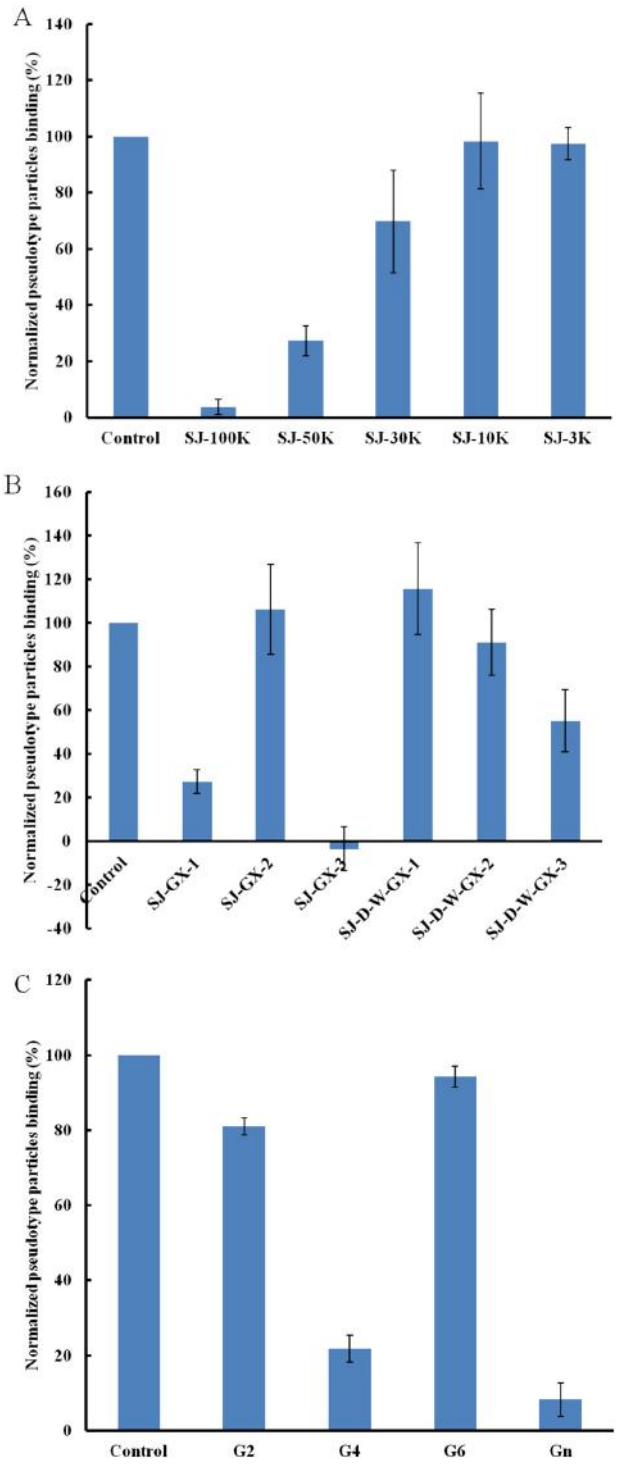


**Fig. 3.** Bar graphs of normalized pseudotype particles binding preference to surface heparin by competing with different modified polysaccharides (mainly on glucuronomannan). Concentration of pseudotype particles was 0.085 mg/mL and concentrations of different polysaccharides were 1000 nM. All bar graphs with standard deviations were based on triplicate experiments.

stable fractions (SJ-GX-3 and SJ-D-W-GX-3) exhibited stronger inhibitory activities than the other two corresponding fractions (Fig. 3B). Monosaccharide analysis indicated that acid-stable fractions (SJ-GX-3 and SJ-D-W-GX-3) were glucuronomannan derivatives, suggesting that glucuronomannan might be one active component to bind the pseudotype particles. A low molecular weight glucuronomannan (Gn) with 7.0 k Da and three glucuronomannan-oligomers were also examined. Gn exhibited very strong inhibitory activity (>90%) (Fig. 3C). It is interesting to

note that glucuronomannan-tetramer showed 78% inhibitory activity.

### 3.4. Kinetics measurements of pseudotype particles interaction with SJ-D-S-H and Gn on heparin chip

Based on the types of polysaccharides from fucose-containing polysaccharides from brown algae [32], a sulfated galactofucan (SJ-D-S-H) and a glucuronomannan (Gn) were further studied. The yields of SJ-D-S-H and Gn from SJ were 3.4% and 0.5%, respectively. We determined the kinetic measurements of the interaction of SJ-D-S-H and Gn with pseudotype particles by solution-based affinities (Ki) and calculated from $IC_{50}$ values from SPR competition experiments. The $IC_{50}$ values of SJ-D-S-H and Gn binding to pseudotype particles are shown in Fig. 4. According to a previous study [11], the dissociation constant ($K_D$) for heparin and pseudotype particles was 0.85 nM (The estimated molecular weight of pseudotype particles is $2.5 \times 10^5$ kDa). Therefore, the Ki of samples were calculated using the equation: $Ki = IC_{50}/(1 + [C]/K_D)$, where [C] is the concentration of pseudotype particles (0.34 nM) used in the competition SPR, and for pseudotype particles binding affinity ($K_D$) for heparin [14,33]. It was shown that the Ki of SJ-D-S-H and Gn binding to pseudotype particles were calculated to be 19 nM and 165 nM, respectively.

### 3.5. Structure features of SJ-D-S-H and Gn

The chemical composition analysis in Fig. 5A indicate that SJ-D-S-H had 21% sulfate, 36% Fuc and 10% Gal, suggesting that the molar ratio of Gal to Fuc in SJ-D-S-H was 0.25: 1. The molar ratio of sulfate residues to Fuc residues was 0.83, using the equation: (sulfate content/103)/(Fuc content/146), where 103 was calculated as $SO_3Na$ and 146 was Fuc-$H_2O$. The molar ratio of sulfate to hexose, including Fuc and Gal was 0.66 calculated using the equation: (sulfate content/103)/(Fuc content/164 + Gal content/162), where 103 was calculated as $SO_3Na$, 162 was Gal-$H_2O$ and 146 was Fuc-$H_2O$. GPC-HPLC shows that SJ-D-S-H had a major peak at 14.090 min, corresponding to the molecular weight of 13.7 kDa and an accompanying shoulder peak (The area ratio of the major peak to the shoulder peak was 1:8) at 11.212 min corresponding to a molecular weight of 195.0 kDa (Fig. 5B). NMR spectroscopy was performed to elucidate the structure of SJ-D-S-H (Fig. 5). Resonances with chemical shifts for anomeric carbons, at 103.0 ppm, are characteristic peaks for 1, 6-linked β-D-Gal residues and β-D-Gal residues, assigned to the residue D and E. These are also confirmed by the presence of two peaks at 62.6 and 72.1 ppm, corresponding to the C6 of β-D-Gal residues and 1, 6-linked β-D-Gal residues, respectively. The chemical shifts at approximately 98.6 ppm are characteristic peaks for

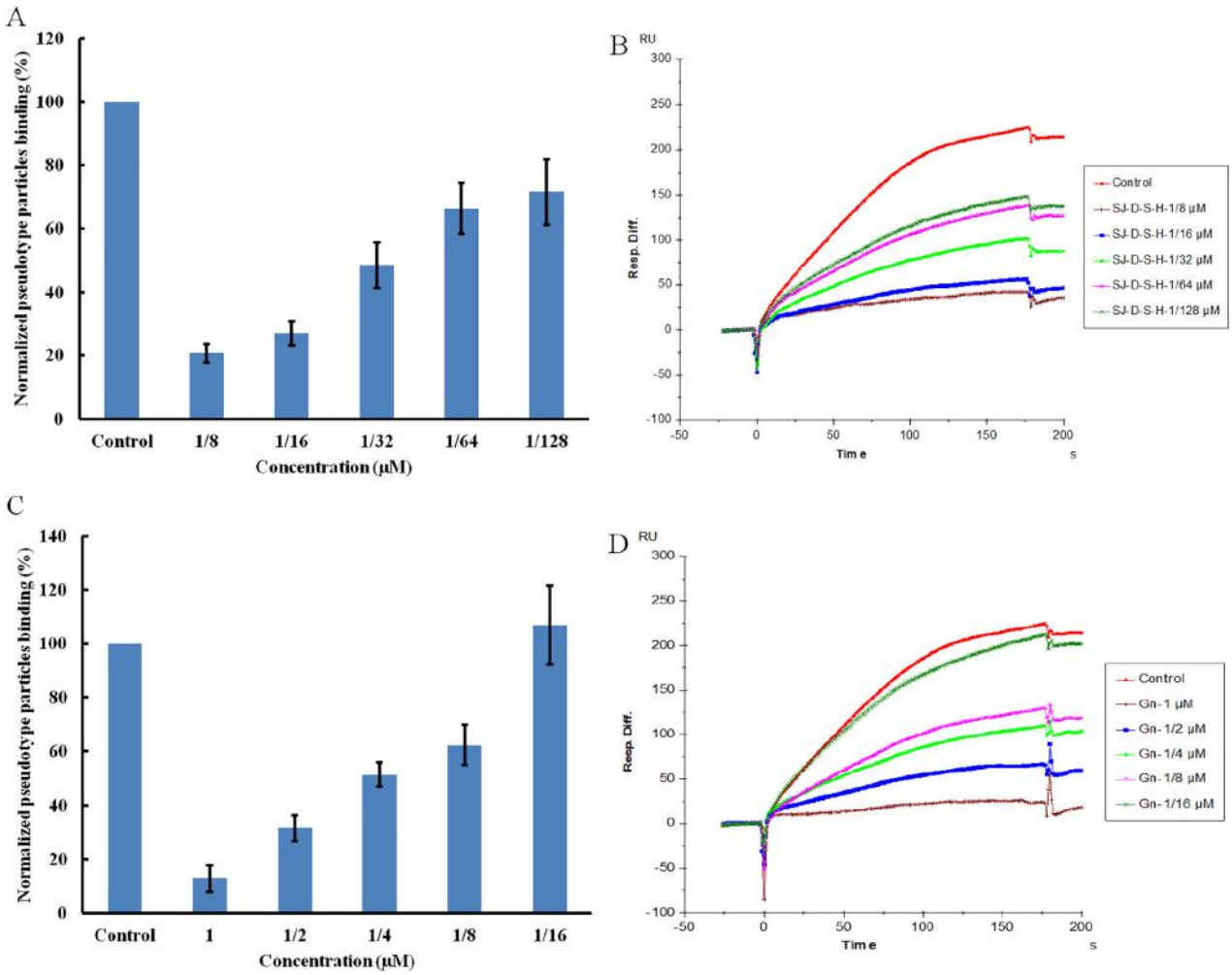


**Fig. 4.** SJ-D-S-H competes with heparin for pseudotype particles (A and B) binding with a $IC_{50}$ of 27 nM and Gn competes with heparin for pseudotype particles (C and D) binding with an $IC_{50}$ of 231 nM. Concentrations were 0.085 mg/mL for pseudotype particles. All bar graphs with standard deviations were based on triplicate experiments.

1, 3-linked α-L-Fuc4S residues, assigned to the residue C. The chemical shifts at approximately 98.0 ppm are characteristic peaks for 1, 3-linked α-L-Fuc2, 4S residues and 1, 3-linked α-L-Fuc4S residues branched at C2 with galacto-biose, corresponding to the residues A and B [22,34–44]. In terms of the $^{1}$H NMR spectrum, resonances with chemical shifts of anomeric protons, at approximately 5.31 ppm, are characteristic peaks for 1, 3-linked α-L-Fuc2, 4S residues (Residue A) and 1,3-linked α-L-Fuc4S residues (Residue B) branched at C2, respectively. The chemical shifts at approximately 5.01 ppm are characteristic peaks for 1, 3-linked α-L-Fuc4S residues (Residue C). The chemical shifts at approximately 4.50 ppm are characteristic peaks for 1, 6-linked β-D-Gal residues (Residue D and E), respectively [34–38]. Moreover, the chemical shifts at 2.12 and 20.3 ppm can be assigned to acetyl groups, indicating that SJ-D-S-H was also acetylated. Two methyl groups at 1.16/1.42 and 2.12 ppm were characteristic of the C6 methyl group of fucose and $CH_3$ of acetyl group, respectively. By comparing these two peak area, it was suggested that the molar ratio of acetyl group to the methyl group of Fuc residues was 0.1 in Fig. 5C. Therefore, based on the above results, we conclude that the primary structure of SJ-D-S-H is 1, 3-linked α-L-Fuc*p* residues sulfated at C4 and C2/C4 and 1, 3-

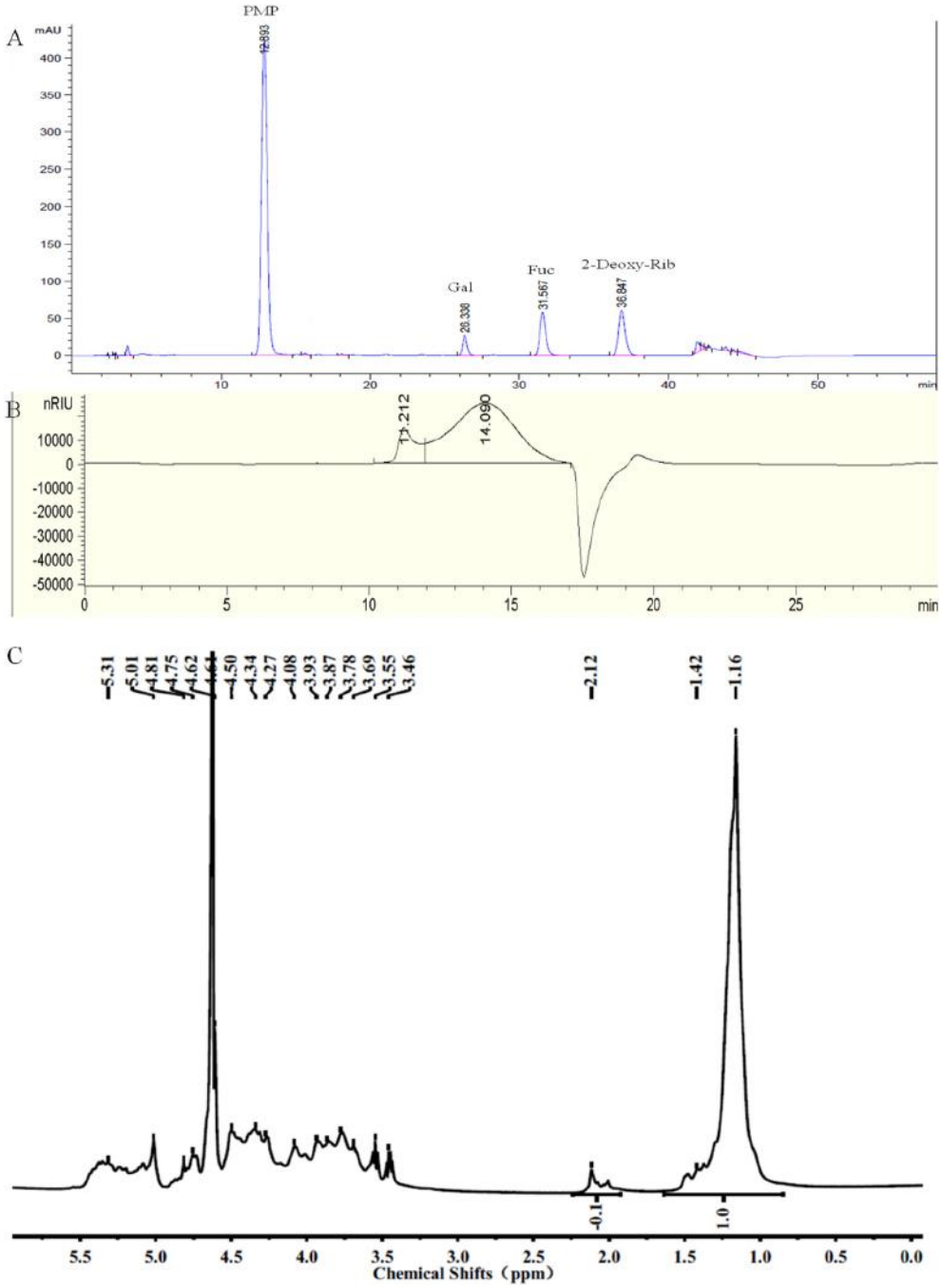


**Fig. 5.** The PMP derivatization-HPLC spectrum (A), GPC-HPLC (B), $^{1}$H NMR spectrum (C), $^{13}$C NMR spectrum (D) and HSQC spectrum (E) for SJ-D-S-H.

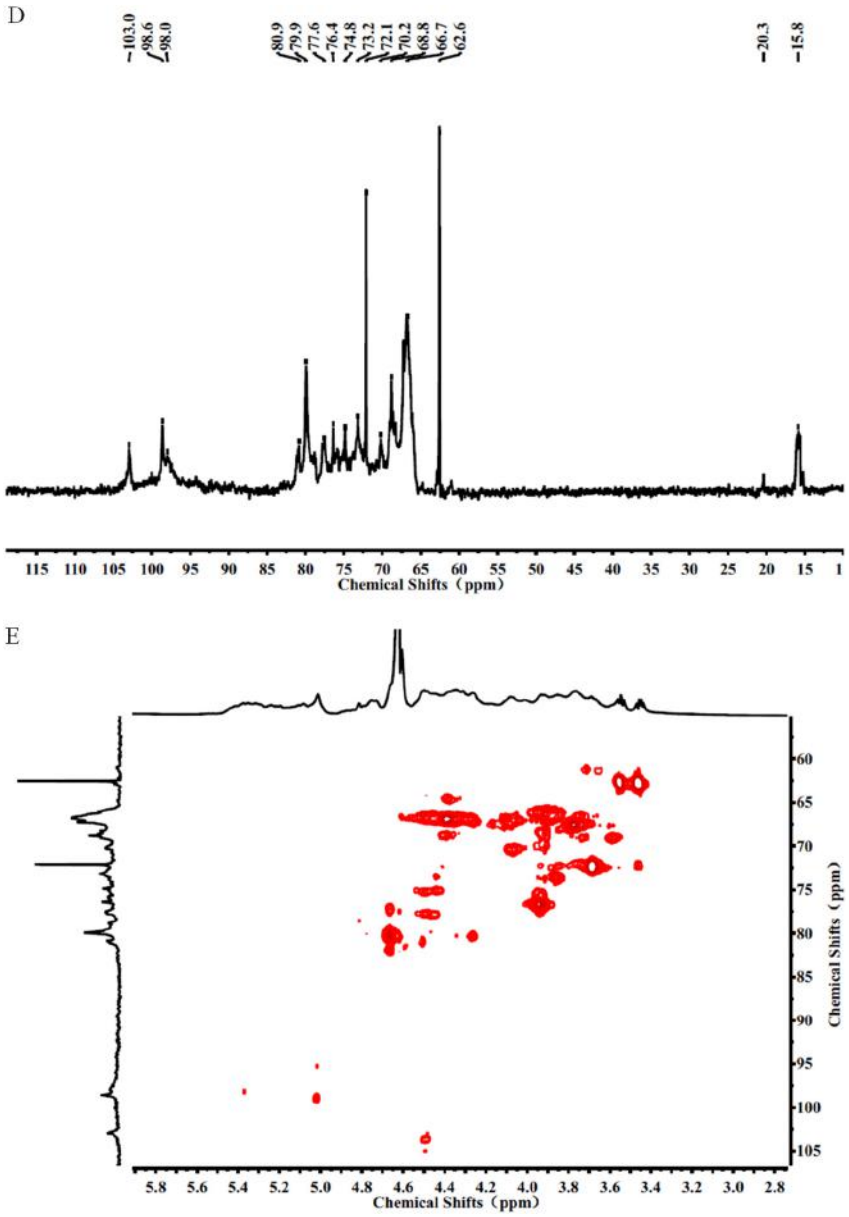


**Fig. 5** (*continued*).

linked α-L-Fuc*p* residues sulfated at C4 and branched with 1, 6-linked β-D-galacto-biose (Fig. 3). In addition, SJ-D-S-H was also randomly substituted with acetyl group and sulfate groups on a small fraction of the Gal residues. The primary structure of SJ-D-S-H is proposed in Fig. 6.

Based on previous studies [25–27,29,45], glucuronomannan (Gn) consists of alternating 1, 4-linked β-D-Glc*Ap* residues and 1, 2-linked α-D-Man*p* residues and has a molecular weight of 7.0 kDa. The primary structure of Gn proposed is shown in Fig. 6.

### *3.6. SPR solution competition study on SARS-CoV-2 spike protein chip of polysaccharides with ACE2*

SARS-CoV-2 SGF binds to ACE2 with high affinity [12]. In our previous study [11], we proposed a model of SARS-CoV-2 attachment and entry, suggesting that virus at first bound to HS in the nasal epithelium glycocalyx, increasing the local concentration of virus, leading to increased infection rates. The HS-virus complex then bound to ACE2 and was endocytosed. In the current study, we show that the sulfated polysaccharides from *S. japonica* exhibited the inhibitory activity between heparin and pseudotype particles containing the SARS-CoV-2 SGPs. Here, we examined whether sulfated polysaccharides could inhibit the interaction between SARS-CoV-2 SGFs and ACE2. SARS-CoV-2 SGFs was immobilized to a CM5 sensor chip to answer this question. ACE2 with or without polysaccharides (or oligosaccharides) was injected over the SARS-CoV-2 spike protein chip to measure the inhibition of polysaccharides on ACE2 binding to SARS-CoV-2 spike protein. ACE2 binds to the SARS-CoV-2 SGP at 140 nM $K_D$ (Fig. 7 and Fig. S1), which is lower than the $K_D$ (15 nM) between SARS-CoV RBD-SD1 and ACE2 [12]. SPR results for polysaccharides showed no or low inhibitory activity on the interaction between SARS-CoV-2 SGPs and ACE2, suggesting that polysaccharides could not inhibit the interaction between SARS-CoV-2 SGPs and ACE2.

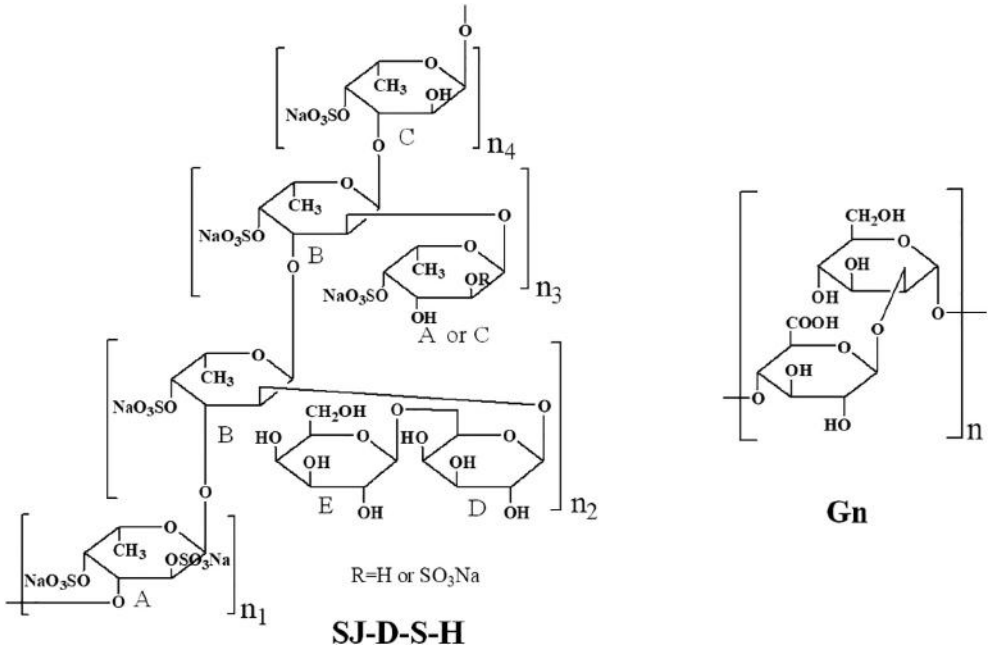


**Fig. 6.** The proposed primary structures of SJ-D-S-H and Gn.

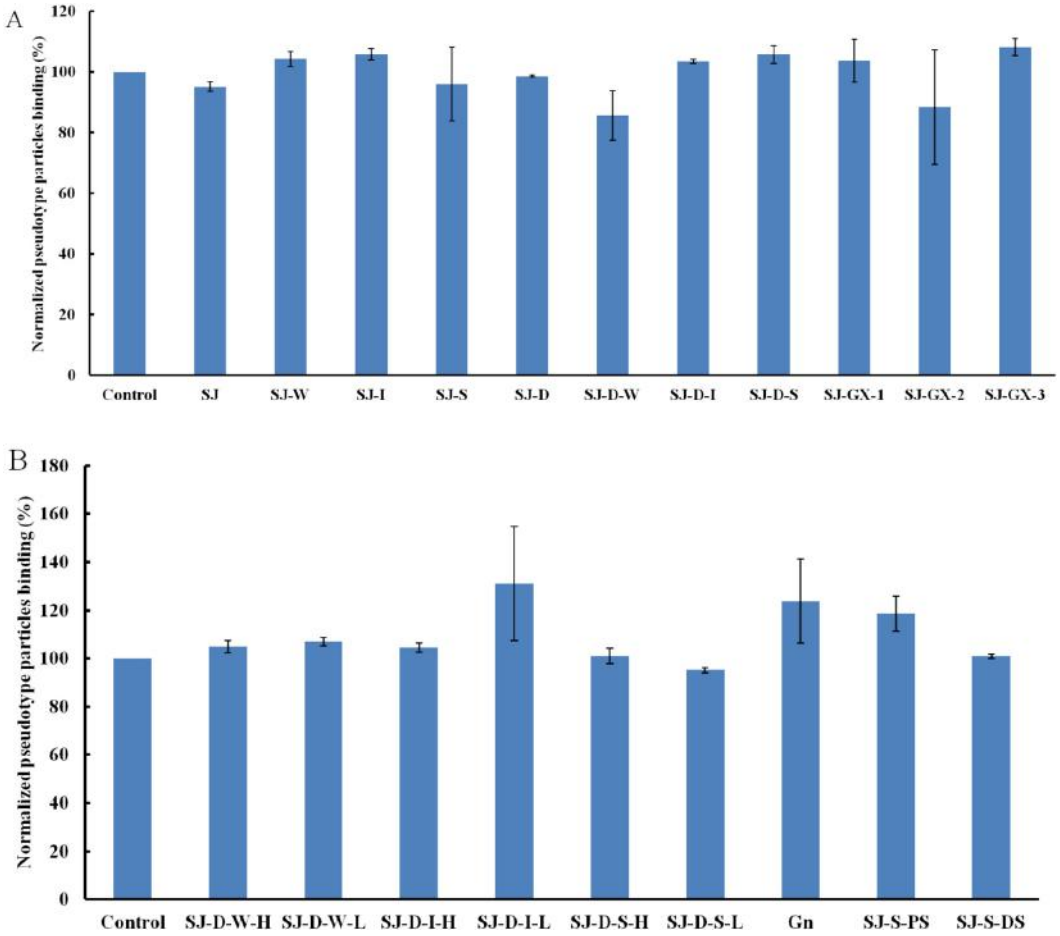


**Fig. 7.** Bar graphs of normalized ACE2 binding preference to surface SARS-CoV-2 spike protein by competing with different polysaccharides. Concentration of ACE2 was 500 nM and concentrations of different polysaccharides were 1000 nM. All bar graphs with standard deviations were based on triplicate experiments.

## 4. Discussion and conclusion

COVID-19 could invade host cell by interacting with host cell surface GAGs through its SGPs [3]. SPR studies confirmed that both monomeric and trimeric SARS-CoV-2 SGPs show very strong binding affinity to heparin, suggesting that heparin had multiple potential targets could be used in COVID-19 therapy [5]. Fucose-containing sulfated polysaccharides (FCSPs) are polysaccharides obtained from brown algae [32,40,46–62]. Sulfated polysaccharides from marine seaweeds have been suggested to have potential antiviral therapeutic activities [63–65]. FCSPs from *Adenocystis utricularis*, *Undaria pinnatifida*, *Stoechospermum marginatum*, *Cystoseira indica*, *Cladosiphon okamuranus* or *Fucus vesiculosus* reportedly exhibit anti-HSV-1, HSV-2, HCMV, VSV, Sindbis virus or HIV-1 by stimulating innate and adaptive immune defense, inhibition of cell adhesion (Stage I), viral replication (Stage II), blockage of the reverse transcriptase (Stage III) [58,62,63,66–73].

Our previous study [6] showed that SJ exhibited promising anti-COVID-19 viral activity *in vitro*. However, SJ was a crude heteropolysaccharide from brown alga *Saccharina japonica*. The structure-activity relationship was studied to find the active components of these polysaccharides. According to the previous studies [32], polysaccharides from brown algae contain sulfated fucan, sulfated galactofucan, fucoglucuronan and fucoglucuronomannan. Anion exchange chromatography was performed to separate SJ and SJ-D into weak (W-type fraction), intermediate (I-type fraction) and strongly (S-type fraction) charged fractions. SPR results indicated that SJ-I and SJ-S had very strong inhibitory activities while only SJ-D-S had very strong inhibitory activity, suggesting that molecular weight also is important for antiviral activity. Selective C2-desulfation was accomplished by autohydrolysis, which is accompanied by partial debranching. Higher molecular weight components (SJ-D-W-H, SJ-D-I-H and SJ-D-S-H) showed stronger inhibitory activities than corresponding low molecular weight components (SJ-D-W-L, SJ-D-I-L and SJ-D-S-L), confirming the above hypothesis. In addition, SJ-D-I-H and SJ-D-S-H showed very strong inhibitory activities. Sulfate content was also examined by preparing desulfated polysaccharides and oversulfated polysaccharides, suggesting that sulfate content was also an important factor. Therefore, we conclude that molecular weight and sulfation level are two important factors, which is consistent with the previous studies [70]. SJ was also degraded using formic acid and separated using five types of ultrafiltration membranes to obtain five different molecular weight fractions. SPR results indicated that the largest molecular weight component ST-100 K, an acid-stable fraction, had the strongest inhibitory activity. Therefore, two concentrations of acid, 0.1 M and 0.5 M HCl, were used to degrade SJ and SJ-D-W to obtain three fractions: (1) dilute acid-sensitive fractions (SJ-GX-1 and SJ-D-W-GX-1); (2) acid-sensitive fractions (SJ-GX-2 and SJ-D-W-GX-2); and (3) acid-stable fractions (SJ-GX-3 and SJ-D-W-GX-3). We found that acid-stable fractions had stronger inhibitory activities than other fractions. Monosaccharide analysis indicated that SJ-GX-3 and SJ-D-W-GX-3 were glucuronomannan derivatives. Three glucuronomannan oligomers (G2, G4 and G6) and one glucuronomannan (Gn) with 7.0 kDa were prepared and their binding to pseudotype particles were determined. The results showed that Gn might be the active component.

In conclusion, polysaccharides from marine seaweeds (Gn and SJ-D-S-H) might represent a good candidate for treatment of COVID-19 based on our systematic study of structure-activity relationship of interaction with SARS-CoV-2 SGPs but not ACE2.

Supplementary data to this article can be found online at https://doi.org/10.1016/j.ijbiomac.2020.09.184.

## CRediT authorship contribution statement

**Weihua Jin**: Conceptualization, Methodology, Data curation, Formal analysis, Funding acquisition, Resources, Writing-Original draft preparation, Project administration; **Wenjing Zhang**: Methodology, Writing-Original draft preparation, Funding acquisition; **Dipanwita Mitra**: Conceptualization, Methodology; **Martin G. McCandless**: Conceptualization, Methodology; **Poonam Sharma**: Conceptualization, Methodology; **Ritesh Tandon**: Conceptualization, Methodology; **Fuming Zhang**: Methodology, Writing Reviewing and Editing; **Robert J. Linhardt**: Writing-Reviewing and Editing.

## Acknowledgements

This study was supported by the Zhejiang Provincial Natural Science Foundation of China (No. LY19D060006), the National Natural Science Foundation of China (No. 41906095) and China Scholarship Council (W.J.). R.T. received funding from National Aeronautics and Space Administration (80NSSC19K1603) and the University of Mississippi Medical Center. The National Institutes of Health Grants DK111958, CA231074, NS088496 and AG062344 to R.J.L.

## References

[1] P. Zhou, X.L. Yang, X.G. Wang, B. Hu, L. Zhang, W. Zhang, H.R. Si, Y. Zhu, B. Li, C.L. Huang, H.D. Chen, J. Chen, Y. Luo, H. Guo, R.D. Jiang, M.Q. Liu, Y. Chen, X.R. Shen, X. Wang, X.S. Zheng, K. Zhao, Q.J. Chen, F. Deng, L.L. Liu, B. Yan, F.X. Zhan, Y.Y. Wang, G.F. Xiao, Z.L. Shi, A pneumonia outbreak associated with a new coronavirus of probable bat origin, Nature 579 (2020) 270–273.

[2] COVID-19 case tracker, https://coronavirus.jhu.edu/#covid-19-basics 2020. (Accessed 22 July 2020).

[3] S.Y. Kim, W. Jin, A. Sood, D.W. Montgomery, O.C. Grant, M.M. Fuster, L. Fu, J.S. Dordick, R.J. Woods, F. Zhang, R.J. Linhardt, Characterization of heparin and severe acute respiratory syndrome-related coronavirus 2 (SARS-CoV-2) spike glycoprotein binding interactions, Antivir. Res. 181 (2020), 104873, .

[4] C. Mycroft-West, D. Su, S. Elli, Y. Li, S. Guimond, G. Miller, J. Turnbull, E. Yates, M. Guerrini, D. Fernig, M. Lima, M. Skidmore, The 2019 coronavirus (SARS-CoV-2) surface protein (Spike) S1 Receptor Binding Domain undergoes conformational change upon heparin binding, BioRxiv (2020)https://doi.org/10.1101/2020.02.29.971093.

[5] U. Lindahl, J.P. Li, Heparin - an old drug with multiple potential targets in Covid-19 therapy, J. Thromb. Haemost. (2020)https://doi.org/10.1111/jth.14898.

[6] P.S. Kwon, H. Oh, S.-J. Kwon, W. Jin, F. Zhang, K. Fraser, J.J. Hong, R.J. Linhardt, J.S. Dordick, Sulfated polysaccharides effectively inhibit SARS-CoV-2 *in vitro*, Cell Discovery 6 (2020) 50.

[7] B.F. Cress, U. Bhaskar, D. Vaidyanathan, A. Williams, C. Cai, X. Liu, L. Fu, M.C. V, F. Zhang, S.A. Mousa, J.S. Dordick, M.A.G. Koffas, R.J. Linhardt, Heavy heparin: a stable isotope-enriched, chemoenzymatically-synthesized, poly-component drug, Angew. Chem. Int. Ed. Eng. 58 (2019) 5962–5966.

[8] Y.P. Lin, Y. Yu, A.L. Marcinkiewicz, P. Lederman, T.M. Hart, F. Zhang, R.J. Linhardt, Non-anticoagulant heparin as a pre-exposure prophylaxis prevents lyme disease infection, ACS Infect. Dis. 6 (2020) 503–514.

[9] N. Nemanichvili, I. Tomris, H.L. Turner, R. McBride, O.C. Grant, R. van der Woude, M.H. Aldosari, R.J. Pieters, R.J. Woods, J.C. Paulson, G.J. Boons, A.B. Ward, M.H. Verheije, R.P. de Vries, Fluorescent trimeric hemagglutinins reveal multivalent receptor binding properties, J. Mol. Biol. 431 (2019) 842–856.

[10] R. Tandon, D. Mitra, P. Sharma, S.J. Stray, J.T. Bates, G.D. Marshall, Effective screening of SARS-CoV-2 neutralizing antibodies in patient serum using lentivirus particles pseudotyped with SARS-CoV-2 spike glycoprotein, MedRxiv (2020)https://doi.org/10.1101/2020.05.21.20108951.

[11] R. Tandon, J.S. Sharp, F. Zhang, V.H. Pomin, N.M. Ashpole, D. Mitra, W. Jin, H. Liu, P. Sharma, R.J. Linhardt, Effective inhibition of SARS-CoV-2 entry by heparin and enoxaparin derivatives, BioRxiv (2020)https://doi.org/10.1101/2020.06.08.140236.

[12] D. Wrapp, N. Wang, K.S. Corbett, J.A. Goldsmith, C.L. Hsieh, O. Abiona, B.S. Graham, J.S. McLellan, Cryo-EM structure of the 2019-nCoV spike in the prefusion conformation, Science 367 (2020) 1260–1263.

[13] W.H. Jin, W.J. Zhang, H.Z. Liang, Q.B. Zhang, The structure-activity relationship between marine algae polysaccharides and anti-complement activity, Mar. Drugs 14 (2016) 3.

[14] W. Jin, D. Jiang, W. Zhang, C. Wang, K. Xia, F. Zhang, R.J. Linhardt, Interactions of fibroblast growth factors with sulfated galactofucan from *Saccharina japonica*, Int. J. Biol. Macromol. 160 (2020) 26–34.

[15] W.H. Jin, J. Wang, H. Jiang, N. Song, W.J. Zhang, Q.B. Zhang, The neuroprotective activities of heteropolysaccharides extracted from *Saccharina japonica*, Carbohydr. Polym. 97 (2013) 116–120.

[16] J. Wang, Q. Zhang, Z. Zhang, Z. Li, Antioxidant activity of sulfated polysaccharide fractions extracted from *Laminaria japonica*, Int. J. Biol. Macromol. 42 (2008) 127–132.

[17] J. Wang, Q. Zhang, Z. Zhang, H. Song, P. Li, Potential antioxidant and anticoagulant capacity of low molecular weight fucoidan fractions extracted from *Laminaria japonica*, Int. J. Biol. Macromol. 46 (2010) 6–12.

[18] W. Jin, H. Tang, J. Zhang, B. Wei, J. Sun, W. Zhang, F. Zhang, H. Wang, R.J. Linhardt, W. Zhong, Structural analysis of a novel sulfated galacto-fuco-xylo-glucurono-mannan from *Sargassum fusiforme* and its anti-lung cancer activity, Int. J. Biol. Macromol. 149 (2020) 450–458.

[19] W. Jin, W. Wu, H. Tang, B. Wei, H. Wang, J. Sun, W. Zhang, W. Zhong, Structure analysis and anti-tumor and anti-angiogenic activities of sulfated galactofucan extracted from *Sargassum thunbergii*, Mar. Drugs 17 (2019) 52.
[20] M. Ciancia, Y. Satob, H. Nonamic, A.S. Cerezod, R. Erra-Balsellsd, M.C. Matulewicz, Autohydrolysis of a partially cyclized mu/nu-carrageenan and structural elucidation of the oligosaccharides by chemical analysis, NMR spectroscopy and UV-MALDI mass spectrometry, Arkivoc xii (2005) 319–331.
[21] R.M. Rodriguez-Jasso, S.I. Mussatto, L. Pastrana, C.N. Aguilar, J.A. Teixeira, Extraction of sulfated polysaccharides by autohydrolysis of brown seaweed *Fucus vesiculosus*, J. Appl. Phycol. 25 (2013) 31–39.
[22] R.V. Menshova, S.D. Anastyuk, S.P. Ermakova, N.M. Shevchenko, V.I. Isakov, T.N. Zvyagintseva, Structure and anticancer activity in vitro of sulfated galactofucan from brown alga *Alaria angusta*, Carbohydr. Polym. 132 (2015) 118–125.
[23] N.M. Shevchenko, S.D. Anastyuk, R.V. Menshova, O.S. Vishchuk, V.I. Isakov, P.A. Zadorozhny, T.V. Sikorskaya, T.N. Zvyagintseva, Further studies on structure of fucoidan from brown alga *Saccharina gurjanovae*, Carbohydr. Polym. 121 (2015) 207–216.
[24] S.D. Anastyuk, T.I. Imbs, N.M. Shevchenko, P.S. Dmitrenok, T.N. Zvyagintseva, ESIMS analysis of fucoidan preparations from *Costaria costata*, extracted from alga at different life-stages, Carbohydr. Polym. 90 (2012) 993–1002.
[25] W. Jin, L. Ren, B. Liu, Q. Zhang, W. Zhong, Structural features of sulfated glucuronomannan oligosaccharides and their antioxidant activity, Mar. Drugs 16 (2018) 291.
[26] W. Jin, J. Wang, S. Ren, N. Song, Q. Zhang, Structural analysis of a heteropolysaccharide from *Saccharina japonica* by electrospray mass spectrometry in tandem with collision-induced dissociation tandem mass spectrometry (ESI-CID-MS/MS), Mar. Drugs 10 (2012) 2138–2152.
[27] W. Jin, X. He, J. Zhu, Q. Fang, W. Bin, J. Sun, W. Zhang, Z. Zhang, F. Zhang, R.J. Linhardt, H. Wang, W. Zhong, Inhibition of glucuronomannan hexamer on the proliferation of lung cancer through binding with immunoglobulin G, Carbohydr. Polym. 248 (2020), 116785, .
[28] W. Jin, W. Zhang, G. Liu, J. Yao, T. Shan, C. Sun, Q. Zhang, The structure-activity relationship between polysaccharides from *Sargassum thunbergii* and anti-tumor activity, Int. J. Biol. Macromol. 105 (2017) 686–692.
[29] J.D. Wu, Y.J. Lv, X.X. Liu, X.L. Zhao, G.L. Jiao, W.J. Tai, P.P. Wang, X. Zhao, C. Cai, G.L. Yu, Structural study of sulfated Fuco-oligosaccharide branched glucuronomannan from *Kjellmaniella crassifolia* by ESI-CID-MS/MS, J. Carbohydr. Chem. 34 (2015) 303–317.
[30] J. Li, F. Gu, C. Cai, M. Hu, L. Fan, J. Hao, G. Yu, Purification, structural characterization, and immunomodulatory activity of the polysaccharides from *Ganoderma lucidum*, Int. J. Biol. Macromol. 143 (2020) 806–813.
[31] W. Zhang, Biotechnology of Glycoconjugated, 2nd ed. Zhejiang University Press, Hangzhou, 1999 91–92.
[32] E. Deniaud-Bouet, K. Hardouin, P. Potin, B. Kloareg, C. Herve, A review about brown algal cell walls and fucose-containing sulfated polysaccharides: cell wall context, biomedical properties and key research challenges, Carbohydr. Polym. 175 (2017) 395–408.
[33] J. Zhao, X. Liu, C. Kao, E. Zhang, Q. Li, F. Zhang, R.J. Linhardt, Kinetic and structural studies of interactions between glycosaminoglycans and langerin, Biochemistry 55 (2016) 4552–4559.
[34] N. Nifantiev, N. Ustyuzhanina, V. Krylov, A. Grachev, A. Gerbst, Synthesis, NMR and conformational studies of fucoidan fragments, 8: convergent synthesis of branched and linear oligosaccharides, Synth 2006 (2006) 4017–4031, https://doi.org/10.1055/s-2006-950333.
[35] D.Z. Vinnitskiy, V.B. Krylov, N.E. Ustyuzhanina, A.S. Dmitrenok, N.E. Nifantiev, The synthesis of heterosaccharides related to the fucoidan from *Chordaria flagelliformis* bearing an alpha-L-fucofuranosyl unit, Org. Biomol. Chem. 14 (2016) 598–611.
[36] J. Zhou, L. Yang, W. Hu, Stereoselective synthesis of a sulfated tetrasaccharide corresponding to a rare sequence in the galactofucan isolated from *Sargassum polycystum*, J. Organomet. Chem. 79 (2014) 4718–4726.
[37] A. Kasai, S. Arafuka, N. Koshiba, D. Takahashi, K. Toshima, Systematic synthesis of low-molecular weight fucoidan derivatives and their effect on cancer cells, Org. Biomol. Chem. 13 (2015) 10556–10568.
[38] C. Zong, Z. Li, T. Sun, P. Wang, N. Ding, Y. Li, Convenient synthesis of sulfated oligofucosides, Carbohydr. Res. 345 (2010) 1522–1532.
[39] M.I. Bilan, A.A. Grachev, A.S. Shashkov, M. Kelly, C.J. Sanderson, N.E. Nifantiev, A.I. Usov, Further studies on the composition and structure of a fucoidan preparation from the brown alga *Saccharina latissima*, Carbohydr. Res. 345 (2010) 2038–2047.
[40] M.I. Bilan, A.A. Grachev, A.S. Shashkov, T.T. Thuy, T.T. Van, B.M. Ly, N.E. Nifantiev, A.I. Usov, Preliminary investigation of a highly sulfated galactofucan fraction isolated from the brown alga *Sargassum polycystum*, Carbohydr. Res. 377 (2013) 48–57.
[41] M.I. Bilan, N.E. Ustyuzhanina, A.S. Shashkov, T.T.T. Thanh, M.L. Bui, T.T.V. Tran, V.N. Bui, N.E. Nifantiev, A.I. Usov, A sulfated galactofucan from the brown alga *Hormophysa cuneiformis* (Fucales, Sargassaceae), Carbohydr. Res. 469 (2018) 48–54.
[42] M.I. Bilan, N.E. Ustyuzhanina, A.S. Shashkov, T.T.T. Thanh, M.L. Bui, T.T.V. Tran, V.N. Bui, A.I. Usov, Sulfated polysaccharides of the Vietnamese brown alga *Sargassum aquifolium* (Fucales, Sargassaceae), Carbohydr. Res. 449 (2017) 23–31.
[43] D. Leal, A. Mansilla, B. Matsuhiro, M. Moncada-Basualto, M. Lapier, J.D. Maya, C. Olea-Azar, W.M. De Borggraeve, Chemical structure and biological properties of sulfated fucan from the sequential extraction of subAntarctic *Lessonia sp* (Phaeophyceae), Carbohydr. Polym. 199 (2018) 304–313.
[44] R.V. Usoltseva, S.D. Anastyuk, N.M. Shevchenko, V.V. Surits, A.S. Silchenko, V.V. Isakov, T.N. Zvyagintseva, P.D. Thinh, S.P. Ermakova, Polysaccharides from brown algae *Sargassum duplicatum*: the structure and anticancer activity *in vitro*, Carbohydr. Polym. 175 (2017) 547–556.
[45] P. Wang, X. Zhao, Y. Lv, Y. Liu, Y. Lang, J. Wu, X. Liu, M. Li, G. Yu, Analysis of structural heterogeneity of fucoidan from *Hizikia fusiforme* by ES-CID-MS/MS, Carbohydr. Polym. 90 (2012) 602–607.
[46] C. Nunes, M.A. Coimbra, The potential of fucose-containing sulfated polysaccharides as scaffolds for biomedical applications, Curr. Med. Chem. 26 (35) (2019) 6399–6411.
[47] O. Berteau, B. Mulloy, Sulfated fucans, fresh perspectives: structures, functions, and biological properties of sulfated fucans and an overview of enzymes active toward this class of polysaccharide, Glycobiology 13 (2003) 29R–40R.
[48] A. Cumashi, N.A. Ushakova, M.E. Preobrazhenskaya, A. D'Incecco, A. Piccoli, L. Totani, N. Tinari, G.E. Morozevich, A.E. Berman, M.I. Bilan, A.I. Usov, N.E. Ustyuzhanina, A.A. Grachev, C.J. Sanderson, M. Kelly, G.A. Rabinovich, S. Iacobelli, N.E. Nifantiev, A comparative study of the anti-inflammatory, anticoagulant, antiangiogenic, and antiadhesive activities of nine different fucoidans from brown seaweeds, Glycobiology 17 (2007) 541–552.
[49] J.H. Fitton, D.N. Stringer, S.S. Karpiniec, Therapies from fucoidan: an update, Mar. Drugs 13 (2015) 5920–5946.
[50] M. Kusaykin, I. Bakunina, V. Sova, S. Ermakova, T. Kuznetsova, N. Besednova, T. Zaporozhets, T. Zvyagintseva, Structure, biological activity, and enzymatic transformation of fucoidans from the brown seaweeds, Biotechnol. J. 3 (2008) 904–915.
[51] B. Li, F. Lu, X. Wei, R. Zhao, Fucoidan: structure and bioactivity, Molecules 13 (2008) 1671–1695.
[52] N.M. Mestechkina, V.D. Shcherbukhin, Sulfated polysaccharides and their anticoagulant activity: a review, Appl. Biochem. Microbiol. 46 (2010) 291–298.
[53] P.A. Mourão, M.S. Pereira, Searching for alternatives to heparin: sulfated fucans from marine invertebrates, Trends Cardiovasc. Med. 9 (1999) 225–232.
[54] R. Pangestuti, S.K. Kim, Neuroprotective effects of marine algae, Mar. Drugs 9 (2011) 803–818.
[55] V.H. Pomin, An overview about the structure-function relationship of marine sulfated homopolysaccharides with regular chemical structures, Biopolym. 91 (2009) 601–609.
[56] K. Senthilkumar, P. Manivasagan, J. Venkatesan, S.K. Kim, Brown seaweed fucoidan: biological activity and apoptosis, growth signaling mechanism in cancer, Int. J. Biol. Macromol. 60 (2013) 366–374.
[57] A.I. Usov, M.I. Bilan, Fucoidans-sulfated polysaccharides of brown algae, Russian Cehem. Rev. 78 (2009) 785–799.
[58] W. Wang, S.-X. Wang, H.-S. Guan, The antiviral activities and mechanisms of marine polysaccharides: an overview, Mar. Drugs 10 (2012) 2795–2816.
[59] I. Wijesekara, R. Pangestuti, S.-K. Kim, Biological activities and potential health benefits of sulfated polysaccharides derived from marine algae, Carbohydr. Polym. 84 (2011) 14–21.
[60] W.A.J.P. Wijesinghe, Y.-J. Jeon, Biological activities and potential industrial applications of fucose rich sulfated polysaccharides and fucoidans isolated from brown seaweeds: a review, Carbohydr. Polym. 88 (2012) 13–20.
[61] G. Jiao, G. Yu, J. Zhang, H. Ewart, Chemical structures and bioactivities of sulfated polysaccharides from marine algae, Mar. Drugs 9 (2011) 196–223.
[62] A.V. Skriptsova, Fucoidans of brown algae: biosynthesis, localization, and physiological role in thallus, Russ. J. Mar. Biol. 41 (2015) 145–156.
[63] Q. Shi, A. Wang, Z. Lu, C. Qin, J. Hu, J. Yin, Overview on the antiviral activities and mechanisms of marine polysaccharides from seaweeds, Carbohydr. Res. 453-454 (2017) 1–9.
[64] L. Pereira, A.T. Critchley, The COVID 19 novel coronavirus pandemic 2020: seaweeds to the rescue? Why does substantial, supporting research about the antiviral properties of seaweed polysaccharides seem to go unrecognized by the pharmaceutical community in these desperate times? J. Appl. Phycol. (2020) 1–3.
[65] C. Sansone, C. Brunet, D.M. Noonan, A. Albini, Marine algal antioxidants as potential vectors for controlling viral diseases, Antioxidants (Basel) 9 (2020) 392.
[66] M.F. de Jesus Raposo, A.M. de Morais, R.M. de Morais, Marine polysaccharides from algae with potential biomedical applications, Mar. Drugs 13 (2015) 2967–3028.
[67] B. Salehi, J. Sharifi-Rad, A.M.L. Seca, D. Pinto, I. Michalak, A. Trincone, A.P. Mishra, M. Nigam, W. Zam, N. Martins, Current trends on seaweeds: looking at chemical composition, phytopharmacology, and cosmetic applications, Molecules 24 (2019) 4182.
[68] P. Mandal, C.G. Mateu, K. Chattopadhyay, C.A. Pujol, E.B. Damonte, B. Ray, Structural features and antiviral activity of sulphated fucans from the brown seaweed *Cystoseira Indica*, Antivir. Chem. Chemother. 18 (2007) 153–162.
[69] K. Hayashi, T. Nakano, M. Hashimoto, K. Kanekiyo, T. Hayashi, Defensive effects of a fucoidan from brown alga *Undaria pinnatifida* against herpes simplex virus infection, Int. Immunopharmacol. 8 (2008) 109–116.
[70] Y. Wang, M. Xing, Q. Cao, A. Ji, H. Liang, S. Song, Biological activities of fucoidan and the factors mediating its therapeutic effects: a review of recent studies, Mar. Drugs 17 (2019) 183.
[71] J.A. Aguilar-Briseno, L.E. Cruz-Suarez, J.F. Sassi, D. Ricque-Marie, P. Zapata-Benavides, E. Mendoza-Gamboa, C. Rodriguez-Padilla, L.M. Trejo-Avila, Sulphated polysaccharides from *Ulva clathrata* and *Cladosiphon okamuranus* seaweeds both inhibit viral attachment/entry and cell-cell fusion, in NDV infection, Mar. Drugs 13 (2015) 697–712.
[72] P. Mohammadi Pour, S. Fakhri, S. Asgary, M.H. Farzaei, J. Echeverría, The signaling pathways, and therapeutic targets of antiviral agents: focusing on the antiviral approaches and clinical perspectives of anthocyanins in the management of viral diseases, Front. Pharmacol. 10 (2019) 1207.
[73] R. Elizondo-Gonzalez, L.E. Cruz-Suarez, D. Ricque-Marie, E. Mendoza-Gamboa, C. Rodriguez-Padilla, L.M. Trejo-Avila, In vitro characterization of the antiviral activity of fucoidan from *Cladosiphon okamuranus* against Newcastle disease virus, Virol. J. 9 (2012) 307.